






Exploring 3P_0 superfluid in dilute spin-polarized neutron matterHiroyuki Tajima ^{1,2}, Hiroshi Funaki ³, Yuta Sekino ^{4,5,6}, Nobutoshi Yasutake ^{7,8} and Mamoru Matsuo ^{3,8,9,10}¹*Department of Physics, Graduate School of Science, The University of Tokyo, Tokyo 113-0033, Japan*²*RIKEN Nishina Center, Wako 351-0198, Japan*³*Kavli Institute for Theoretical Sciences, University of Chinese Academy of Sciences, Beijing 100190, China*⁴*RIKEN Cluster for Pioneering Research (CPR), Astrophysical Big Bang Laboratory (ABBL), Wako, Saitama 351-0198 Japan*⁵*Interdisciplinary Theoretical and Mathematical Sciences Program (iTHEMS), RIKEN, Wako, Saitama 351-0198, Japan*⁶*Nonequilibrium Quantum Statistical Mechanics RIKEN Hakubi Research Team, RIKEN Cluster for Pioneering Research (CPR), RIKEN iTHEMS, Wako, Saitama 351-0198, Japan*⁷*Department of Physics, Chiba Institute of Technology (CIT), 2-1-1 Shibazono, Narashino, Chiba 275-0023, Japan*⁸*Advanced Science Research Center, Japan Atomic Energy Agency, Tokai 319-1195, Japan*⁹*CAS Center for Excellence in Topological Quantum Computation, University of Chinese Academy of Sciences, Beijing 100190, China*¹⁰*RIKEN Center for Emergent Matter Science (CEMS), Wako, Saitama 351-0198, Japan*

(Received 5 June 2023; accepted 7 November 2023; published 29 November 2023)

We explore the theoretical possibility of 3P_0 neutron superfluid in dilute spin-polarized neutron matter, which may be relevant to the crust region of a magnetized neutron star. In such a dilute regime where the neutron Fermi energy is less than 1 MeV, the 1S_0 neutron superfluid can be suppressed by a strong magnetic field of the compact star. In the low-energy limit relevant for dilute neutron matter, the 3P_0 interaction is stronger than the 3P_2 one which is believed to induce the triplet superfluid in the core. We present the ground-state phase diagram of dilute neutron matter with respect to the magnetic field and numerically estimate the critical temperature of the 3P_0 neutron superfluid, which is found to exceed 10^7 K.

DOI: [10.1103/PhysRevC.108.L052802](https://doi.org/10.1103/PhysRevC.108.L052802)

Introduction. A recent progress of neutron-star observations gives us an important opportunity to examine the exotic state of matter such as nucleon superfluidity. The cooling process of neutron stars and pulsar glitch phenomena have been studied in connection with the neutron superfluidity [1]. In the neutron-star crust region with the subnuclear density, the 1S_0 neutron superfluid has been discussed extensively [2] (see also recent review [3]). On the other hand, in the core region of neutron stars where the nucleon density is close to the normal nuclear density $\rho_0 = 0.16 \text{ fm}^{-3}$, the 3P_2 neutron superfluid is expected to occur based on the nucleon-nucleon phase shift at relevant energies with respect to the neutron Fermi energy therein [4]. Based on the recent rapid progress of multimessenger astronomy observations [5], such nuclear many-body states can be further studied in various astrophysical environments in the future, as the observed rapid cooling of Cassiopeia A implies the existence of 3P_2 neutron superfluid [6].

The strong magnetic field in magnetars may lead to non-trivial effects not yet to be revealed (e.g., appearances of spin-3/2 Δ baryons [8] and superheavy nuclei [9]). Magnetars may involve a strong magnetic field $B \approx 10^{15-18}$ G as studied in recent works, e.g., Refs. [10–12]. In particular, the deformation of the magnetar observed via x-ray spectra indicates the existence of an extreme toroidal magnetic field B_t [13], which is stronger than the dipole one B_d estimated from the spin-down luminosity. The resulting Zeeman shift $h = |\gamma_n B|/2 \lesssim 10$ MeV with the neutron gyromagnetic ratio $\gamma_n = -1.2 \times 10^{-17}$ MeV/G is small compared to the neutron Fermi energy E_F around $\rho = \rho_0$, where $E_F = \frac{(3\pi^2\rho)^{2/3}}{2M} \simeq 60$ MeV

(where $M = 939$ MeV is the neutron mass) [3]. This fact evinces that the 1S_0 neutron superfluid without the spin polarization should be dominant at subnuclear densities. However, it is not necessarily true in the dilute region where neutrons just started to drip from neutron-rich nuclei in the inner crust [14]. At a smaller density $\rho = 10^{-3}\rho_0$ (near the neutron drip density), one obtains $E_F \simeq 0.6$ MeV, which can be comparable with the Zeeman shift h . As a result, 1S_0 pairing gap $\Delta_{1S_0} \ll E_F$ can be strongly suppressed by h [15].

In such a dilute region, the low-energy nucleon-nucleon phase shift shown in Fig. 1 is important. One can see that 1S_0 channel is dominant at low energies ($E_{\text{lab}} \lesssim 150$ MeV where E_{lab} is the laboratory kinetic energy). However, suppose that dilute neutron matter is polarized due to the strong magnetic field, the dominant attractive interactions turn to be the triplet P -wave channels, that is, 3P_0 and 3P_2 . Interestingly, the 3P_0 channel can be a leading contribution near the drip density ($E_{\text{lab}} \lesssim 100$ MeV as shown in Fig. 1) in contrast to the core region of neutron stars ($E_{\text{lab}} \lesssim 150$ MeV corresponding to $E_F \gg h$) where the 3P_2 channel is relevant [16].

In this work, we theoretically explore the possibility of 3P_0 neutron superfluid in dilute spin-polarized neutron matter, which may be relevant to the crust region near the neutron drip line under the strong magnetic field. First, we consider the possible ground-state phase diagram in terms of the magnetic field and the neutron density. Because we are interested in the dilute regime where the low-energy universality is relevant, we utilize the recent theoretical results of strongly interacting Fermi gases near the unitary limit [17–19] to characterize 1S_0

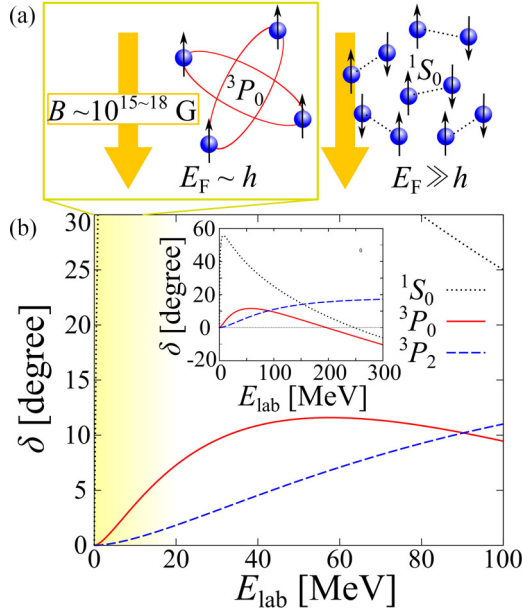


FIG. 1. (a) Schematics of 3P_0 neutron superfluid in dilute neutron matter with a large spin polarization due to the magnetic field B where the Zeeman shift h is comparable with the Fermi energy E_F . At larger densities where $E_F \gg h$, the 1S_0 neutron superfluid without the spin polarization can appear. (b) Low-energy nucleon-nucleon phase shift of the isovector channel from the Nijmegen partial wave analysis (NPWA) [7], where E_{lab} is the laboratory kinetic energy. The inset shows the phase shift with the relatively high-energy regime (≈ 300 MeV). In the dilute region with $E_F \sim h$ (shaded area), 3P_0 scattering phase shift can be a relevant channel for spin-polarized neutron matter.

superfluid properties with largely negative scattering length $a = -18.5$ fm. In such a way, we identify the possible spin-polarized regime at zero temperature. Moreover, we develop the mean-field framework of 3P_0 neutron superfluid. The separable interaction is employed to reproduce the 3P_0 scattering amplitude. Finally, we predict the critical temperature of 3P_0 superfluid as a function of a spin-polarized neutron density.

Hereafter, we use the units of $\hbar = k_B = c = 1$ and the system volume is taken to be unity for convenience.

Ground-state phase diagram. First, we qualitatively examine the possible ground-state phase diagram in dilute neutron matter under the strong magnetic field. To this end, the information of strongly interacting Fermi gases near the unitary limit is useful [17–19]. In the dilute system with the negligible finite-range effect [20], the relevant energy scale for the 1S_0 neutron superfluid is given by $1/(Ma^2) = 0.12$ MeV with $a = -18.5$ fm. In this regard, the Zeeman shift $h \lesssim 10$ MeV is not necessarily negligible in the dilute region. Based on the theoretical study of spin-imbalanced Fermi gases [21], the saturation Zeeman shift h_s beyond which neutrons are fully polarized is expressed in terms of the attractive Fermi polaron energy $E_P < 0$ as [see also Fig. 2(a)]

$$h_s = \frac{E_F + |E_P|}{2}. \quad (1)$$

Note that E_P has been determined precisely in strongly interacting ultracold Fermi gases [22,23] (for review, see,

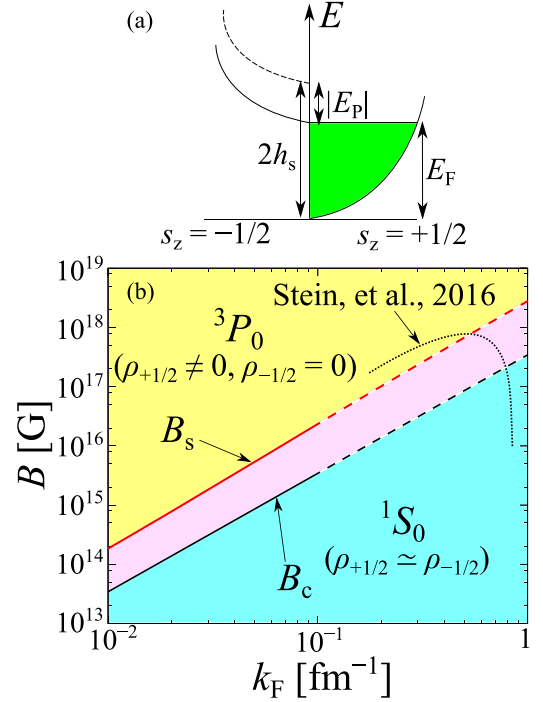


FIG. 2. (a) Energy diagram of spin-1/2 neutrons (left: $s_z = -1/2$, right: $s_z = +1/2$) at the saturation Zeeman shift $h = h_s$. While the $s_z = -1/2$ neutrons exhibit the polaron energy shift E_P with respect to the bare dispersion (dashed line), $s_z = +1/2$ neutrons form the Fermi sea with the Fermi energy E_F . Below $h = h_s$, the $s_z = -1/2$ state starts to be occupied. (b) Schematic ground-state phase diagram of dilute neutron matter under the strong magnetic field B . k_F is the Fermi momentum. B_s denotes the saturation magnetic field beyond which neutron matter is fully polarized. B_c is the critical magnetic field for the 1S_0 superfluid. For comparison, the unpaired magnetic field in the mean-field calculation with the multirank separable interaction at $T = 0.05$ MeV (Stein *et al.*, 2016 [15]) is also plotted (dotted curve). In the high-density region ($k_F \lesssim 0.1$ fm $^{-1}$), where the dashed lines are plotted, our results are not quantitatively valid due to the finite-range effect.

e.g., [24–26]). For a given density $\rho_{+1/2}$ of spin $s_z = +1/2$ neutrons, where the direction of B is parallel with $s_z = -1/2$, the G -matrix calculation with the contact-type interaction reads [27,28]

$$E_P = \frac{\rho_{+1/2}}{4\pi a - \frac{Mk_F}{2\pi^2}} = -\frac{2}{3}E_F \frac{1}{1 - \frac{\pi}{2}(k_F a)^{-1}}, \quad (2)$$

which gives $E_P \simeq -0.67E_F$ at unitarity [i.e., $(k_F a)^{-1} = 0$]. Regardless of its simple calculation, this value is consistent with the experimental value $E_P = -0.64(7)E_F$ [22]. In the dilute limit, one obtains $E_P/E_F = \frac{4\pi a}{M} \rho_{+1/2}/E_F = \frac{4}{3\pi}(k_F a)$, reproducing the Hartree shift. We note that the finite-range effect in the nucleon-nucleon interaction can enlarge E_P as $E_P \simeq 0.75E_F$ at $k_F \simeq 1$ fm $^{-1}$ [29]. A similar tendency can also be found in the case of polaronic protons in neutron matter [30]. Eventually, the saturation magnetic field reads

$$B_s = \frac{E_F}{|\gamma_n|} \left[1 + \frac{2}{3} \frac{1}{1 - \frac{\pi}{2}(k_F a)^{-1}} \right]. \quad (3)$$

Also, the Chandrasekhar-Clogston limit reads $2h_c/\mu_c \simeq 1.09$ [31,32], where h_c and μ_c are the critical values of the Zeeman shift and the chemical potential, respectively. For simplicity, we take $\mu_c \simeq \xi_B E_F$, where $\xi_B \simeq 0.37$ is the Bertsch parameter [33–35]. Resulting $h_c \simeq 0.2E_F \equiv |\gamma_n B_c|/2$ gives a reasonable estimation around unitarity compared to the diagrammatic approach [36]. Because of anisotropic scattering in polarized matter, the Fermi sea may be deformed. Even in such a case, the Fermi polaron energy can be calculated as in Ref. [37].

Figure 2(b) shows the ground-state phase diagram of dilute neutron matter with respect to k_F and B . Above $B = B_s$, the system is fully polarized and therefore the 3P_0 neutron superfluid can be a possible ground state in this region. On the other hand, below $B = B_c$ the system is expected to be well-studied 1S_0 neutron superfluid phase. Suppose that the possible magnetic field reach $B \approx 10^{15-18}$ G inside of the compact stars [38], one may expect the spin-polarized 3P_0 neutron superfluid phase in the dilute region at $k_F \lesssim 1 \text{ fm}^{-1}$. For comparison, the mean-field result with the separable interaction for the unpaired magnetic field at $T = 0.05 \text{ MeV}$ [15] is plotted. On the one hand, it is larger than B_c at low densities. This may originate from the difference of theoretical frameworks, where we have estimated B_c by using the results of cold-atom experiments, while the mean-field approximation was employed in Ref. [15]. Indeed, the mean-field calculation overestimates the critical magnetic field in a strongly interacting regime [39]. On the other hand, the result of Ref. [15] drops to zero around $k_F = 0.8 \text{ fm}^{-1}$, indicating the importance of the finite-range properties of the interaction. Because our approach is based on cold atomic physics, where the finite-range effect is negligible, our result is quantitatively valid in the low-density region $k_F \ll r_{\text{eff}}^{-1} \simeq 0.36 \text{ fm}^{-1}$ (where $r_{\text{eff}} = 2.8 \text{ fm}$ is the 1S_0 effective range [40]). In this regard, we used the dashed lines at $k_F \lesssim 0.1 \text{ fm}^{-1}$ in Fig. 2(b). In the region between B_s and B_c , the ground state picture is elusive as various possibilities such as Sarma phase [41], Fulde-Ferrel-Larkin-Ovchinnikov superfluid [42,43], induced P -wave pairing [44], and spin polarized droplet [45,46] were discussed (for a review see Refs. [47,48]). Since we are interested in the fully spin-polarized phase, we do not go into details about this region. However, if there exists the spin-polarized component, 3P_0 superfluid may appear in such a regime. We note that the 3P_2 superfluid phase is not shown in Fig. 2(b) because it is expected to be found at larger densities [2,16].

3P_0 neutron superfluid theory. We consider a neutron matter with spin-triplet 3P_0 interaction where the Hamiltonian is given by $H = K + V_{3P_0}$. The kinetic term K of neutrons with the spin $s_z = \pm 1/2$, the mass $M = 939 \text{ MeV}$, and the chemical potential μ reads

$$K = \sum_{\mathbf{k}} \sum_{s_z = \pm 1/2} \left(\frac{k^2}{2M} - \mu - 2s_z h \right) c_{\mathbf{k}, s_z}^\dagger c_{\mathbf{k}, s_z} \\ \simeq \sum_{\mathbf{k}} \left(\frac{k^2}{2M} - \mu - h \right) c_{\mathbf{k}, +1/2}^\dagger c_{\mathbf{k}, +1/2}. \quad (4)$$

In Eq. (4), we ignored the $s_z = -1/2$ component by assuming the large Zeeman shift $h = |\gamma_n B|/2 > h_s$, where the direction of B is taken to be antiparallel with respect to $s_z = +1/2$.

For convenience, we define the z projection of the two-neutron pair spin $S_z = s_z + s'_z$ and the total angular momentum $J_z = S_z + m$. The 3P_0 interaction ($S=1, \ell=1, J=0$) is given by

$$V_{3P_0} = 2\pi \sum_{\mathbf{k}, \mathbf{k}', \mathbf{P}} \sum_m \sum_{s_z, s'_z} V(k, k') Y_{1,m}(\hat{\mathbf{k}}) Y_{1,m}^*(\hat{\mathbf{k}}') \\ \times \langle 1, m; 1, S_z | 0, J_z \rangle \langle s_z, s'_z; s, s_z | 1, S_z \rangle^2 \\ \times c_{\mathbf{k}+\mathbf{P}/2, s_z}^\dagger c_{-\mathbf{k}+\mathbf{P}/2, s'_z}^\dagger c_{-\mathbf{k}+\mathbf{P}/2, s'_z} c_{\mathbf{k}+\mathbf{P}/2, s_z}, \quad (5)$$

where $\langle \ell, m; S, S_z | J, J_z \rangle$ is the Clebsch-Gordan coefficient. For the spin-polarized dilute neutron matter, we consider the 3P_0 interaction between two neutrons with the parallel spins (i.e., $s_z = s'_z = +1/2$) at zero center-of-mass momentum ($\mathbf{P} = \mathbf{0}$) as

$$V_{3P_0} \simeq 2\pi \sum_{\mathbf{k}, \mathbf{k}'} V(k, k') \left[\frac{1}{3} Y_{1,-1}(\hat{\mathbf{k}}) Y_{1,-1}^*(\hat{\mathbf{k}}') \right] \\ \times c_{\mathbf{k}, 1/2}^\dagger c_{-\mathbf{k}, 1/2}^\dagger c_{-\mathbf{k}', 1/2} c_{\mathbf{k}', 1/2}. \quad (6)$$

Furthermore, we use the separable interaction $V(k, k') = g\gamma_k \gamma_{k'}$ ($g < 0$). The superfluid order parameter is introduced as

$$\Delta_{\mathbf{k}} = \gamma_{\mathbf{k}} \frac{k_x - ik_y}{\sqrt{2}k} d, \quad (7)$$

where

$$d = -g \sum_q \frac{q_x + iq_y}{\sqrt{2}q} \gamma_q \langle c_{-q, 1/2} c_{q, 1/2} \rangle. \quad (8)$$

Using Eqs. (7) and (8), we obtain the mean-field Hamiltonian

$$H_{\text{MF}} = \frac{1}{2} \sum_{\mathbf{k}} \Psi_{\mathbf{k}}^\dagger \begin{pmatrix} \xi_{\mathbf{k}, +1/2} & -\Delta_{\mathbf{k}} \\ -\Delta_{\mathbf{k}}^* & -\xi_{\mathbf{k}, +1/2} \end{pmatrix} \Psi_{\mathbf{k}} \\ - \frac{|d|^2}{2g^2} + \frac{1}{2} \sum_{\mathbf{k}} \xi_{\mathbf{k}, +1/2}, \quad (9)$$

where $\Psi_{\mathbf{k}} = (c_{\mathbf{k}, +1/2} \ c_{-\mathbf{k}, +1/2}^\dagger)^T$ is the two-component Nambu spinor and $\xi_{\mathbf{k}, +1/2} = k^2/2M - \mu - h$. Accordingly, the Nambu-Gor'kov Green's function is given by $\hat{G}(\mathbf{k}, i\omega_n) = [i\omega_n - \xi_{\mathbf{k}, +1/2} \tau_3 + \text{Re}(\Delta_{\mathbf{k}}) \tau_1 - \text{Im}(\Delta_{\mathbf{k}}) \tau_2]^{-1}$, where $\tau_{1,2,3}$ is the Pauli matrix, $\omega_n = (2n+1)\pi T$ is the fermion Matsubara frequency ($n \in \mathbb{Z}$), and $E_{\mathbf{k}} = \sqrt{\xi_{\mathbf{k}, +1/2}^2 + |\Delta_{\mathbf{k}}|^2}$ is the quasiparticle dispersion. The gap equation is obtained from $d = gT \sum_q \sum_{i\omega_n} \frac{q_x + iq_y}{\sqrt{2}q} \gamma_q G_{12}(\mathbf{q}, i\omega_n)$, which can be rewritten as

$$1 = -g \sum_q \frac{q_x^2 + q_y^2}{2q^2} \frac{\gamma_q^2}{2E_q} \tanh\left(\frac{E_q}{2T}\right). \quad (10)$$

By solving Eq. (10), one can examine the 3P_0 superfluid properties in spin-polarized neutron matter.

We note that the present 3P_0 neutron superfluid with momentum-dependent gap $\Delta_{\mathbf{k}} \propto k_x - ik_y$ ($\Delta_{\mathbf{k}}^* \propto k_x + ik_y$) is similar to the gapless $p_x + ip_y$ Fermi superfluid predicted in cold atoms [49] as well as the A_1 phase in ${}^3\text{He}$ superfluids [50–52]. Indeed, the gapless points (called the Weyl

nodes or the Fermi points) can be found at $E_k = 0$, that is, $\mathbf{k} = (0, 0, \pm\sqrt{2M(\mu + \hbar)})$ in the momentum space [53]. Thus, if the 3P_0 superfluid is present, the superfluid spin edge current may flow accompanying the chiral anomaly around the surface of uniform neutron matter. Moreover, the 3P_0 gap structure leads to an anisotropic spin response, which may induce a characteristic spin transport at the interfaces with other phases (e.g., 1S_0 superfluid) as in the case of superconducting materials [54–56]. Another important consequence of the 3P_0 superfluid can be found in the specific heat C , which plays a crucial role in the thermal transport during the cooling process [57]. Because of the gapless quasiparticle excitation, $C \propto T^3$ can be found at low temperature [58]. Also, the pair-breaking formation process associated with 3P_0 superfluid might occur in the cooling process [59]. The topological aspects of 3P_0 superfluid and associated vortices can be further examined as in the case of 3P_2 superfluid in the core region [16,60,61].

Next, we relate the model parameters with the 3P_0 scattering amplitude $f_{3P_0}(k) = k^2(-v^{-1} + \frac{1}{2}rk^2 - ik^3)^{-1}$, where v and r are the scattering volume and the effective range, respectively. These low-energy constants are given by $v = -2.638 \text{ fm}^3$ and $r = 3.182 \text{ fm}^{-1}$ [62,63]. The two-body T -matrix reads [64]

$$T(\mathbf{p}, \mathbf{p}'; \omega) = \bar{V}(\mathbf{p}, \mathbf{p}') + \sum_{\mathbf{q}} \frac{\bar{V}(\mathbf{p}, \mathbf{q})T(\mathbf{q}, \mathbf{p}'; \omega)}{\omega_+ - q^2/M_v} \quad (11)$$

with $\omega_+ = \omega + i\eta$ (η is an infinitesimally small value) and $\bar{V}(\mathbf{p}, \mathbf{p}') = \frac{4\pi}{3}g\gamma_p\gamma_{p'}Y_{1,-1}(\hat{\mathbf{p}})Y_{1,-1}^*(\hat{\mathbf{p}}')$. The separability of the T -matrix leads to the form given by $T(\mathbf{p}, \mathbf{p}'; \omega) = \frac{4\pi}{3}t(\omega)\gamma_p\gamma_{p'}Y_{1,-1}(\hat{\mathbf{p}})Y_{1,-1}^*(\hat{\mathbf{p}}')$, where $t(\omega) = g[1 - g\Pi(\omega)]^{-1}$. The pair propagator $\Pi(\omega)$ is given by

$$\Pi(\omega) = \sum_{\mathbf{q}} \frac{4\pi}{3} \gamma_q^2 Y_{1,-1}^*(\hat{\mathbf{q}}) Y_{1,-1}(\hat{\mathbf{q}}) \frac{1}{\omega_+ - q^2/M}. \quad (12)$$

For simplicity, we employ $\gamma_q = \frac{q}{1+(q/\Lambda)^2}$. In this case, we obtain

$$\Pi(\omega) = -\frac{iM\Lambda^4(2\sqrt{M\omega_+} + i\Lambda)(\sqrt{M\omega} - i\Lambda)^2}{24\pi(M\omega + \Lambda^2)^2}. \quad (13)$$

Using this, we find the scattering amplitude $f_{3P_0}(k) = k^2 \left[\frac{12\pi(k^2 + \Lambda^2)^2}{Mg\Lambda^4} + \frac{i(2k+i\Lambda)(k-i\Lambda)^2}{2} \right]^{-1}$. In this way, we find the condition for g and Λ as $v^{-1} = \frac{12\pi}{M} \left(\frac{1}{g} + \frac{M\Lambda^3}{24\pi} \right)$, $r = -\frac{24\pi}{M} \left(\frac{2}{g\Lambda^2} + \frac{M\Lambda}{8\pi} \right) = -\frac{48\pi}{gM\Lambda^2} - 3\Lambda$. For $v = -2.638 \text{ fm}^3$ and $r = 3.182 \text{ fm}^{-1}$, we obtain $\Lambda = 0.63058 \text{ fm}^{-1}$ and $Mg = -74.745 \text{ fm}^3$.

Critical temperature of 3P_0 superfluid. The superfluid critical temperature T_c is an important quantity to examine the possible appearance of the 3P_0 neutron superfluid in an astrophysical environment. We can calculate T_c by taking $T \rightarrow T_c$ and $d \rightarrow 0$ in Eq. (10) as

$$1 = -\frac{Mg}{6\pi^2} \int_0^\infty q^2 dq \frac{\gamma_q^2}{2M\xi_{q,+1/2}} \tanh\left(\frac{\xi_{q,+1/2}}{2T_c}\right). \quad (14)$$

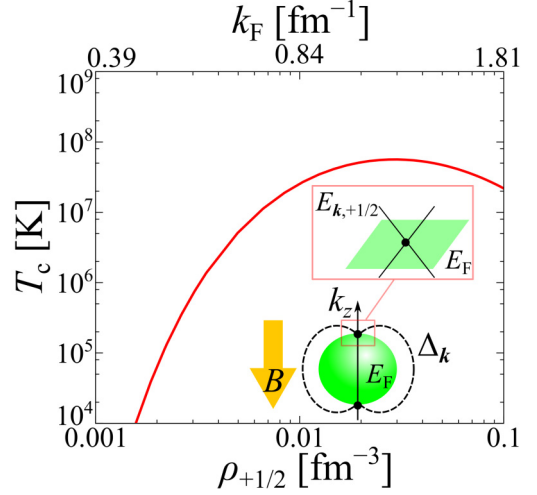


FIG. 3. Critical temperature T_c of 3P_0 neutron superfluidity exhibiting the Weyl nodes at $\mathbf{k} = (0, 0, \pm\sqrt{2M(\mu + \hbar)})$ as a function of the spin $s_z = +1/2$ neutron density $\rho_{+1/2}$. For reference, we show the corresponding neutron Fermi momenta $k_F = (6\pi^2\rho_{+1/2})^{1/3}$ above.

Equation (14) should be solved together with the number density equation [65]

$$\rho_{+1/2} = \frac{1}{4\pi^2} \int_0^\infty k^2 dk \left[1 - \tanh\left(\frac{\xi_{k,+1/2}}{2T_c}\right) \right]. \quad (15)$$

Figure 3 shows the calculated critical temperature T_c of 3P_0 neutron superfluidity as a function of $\rho_{+1/2}$. T_c reaches 10^7 K around $\rho_{+1/2} \simeq 0.01 \text{ fm}^{-3}$. This temperature can be realized in old neutron stars [66]. Although the temperature in a magnetar is typically larger than those of old stars [67], $T \approx 10^7$ K may be not so unrealistic. In this regard, we need to carefully consider the magnetic field and the temperature in neutron stars to explore the possible candidates of stars involving 3P_0 neutron superfluidity. The suitable condition for 3P_0 superfluid would be $B > B_s$ and $T < T_c$. It should be noted that the density region in Fig. 3 is beyond the regime where the zero-range approximation for the 1S_0 channel in Fig. 2 is quantitatively valid (i.e., $k_F \ll 0.36 \text{ fm}^{-1}$). In this sense, further quantitative investigation of B_s with the finite-range 1S_0 interaction is needed. Nevertheless, T_c in Fig. 3 would be useful once spin-polarized neutron matter is realized. On the other hand, it may be not so straightforward to precisely determine the profiles of T and B inside stars [10]. As three-dimensional evolution of the magnetic field has been studied by the magneto-hydrodynamic simulations recently [12], the survey of the regime satisfying this condition by combining the recent observations and simulations would be left as an interesting future work.

We note that while we employ the mean-field approximation to calculate T_c of 3P_0 superfluid, this calculation can be justified in the 3P_0 channel because the 3P_0 interaction strength itself is not so strong as we can see its phase shift in Fig. 1, which is much smaller than the 1S_0 one. Moreover, in the dilute region, the density and spin fluctuations are not crucial

compared to those in the dense region as found in the 1S_0 channel [68].

Summary. In this work, we have theoretically discussed the possible appearance of 3P_0 neutron superfluid, which was overlooked in the literature, in dilute neutron matter with the large spin polarization under the strong magnetic field. For the ground state at $T = 0$, we qualitatively clarified the spin-polarized 3P_0 superfluid phase in the phase diagram with respect to the magnetic field B and the Fermi momentum k_F in the dilute regime. After developing the superfluid theory for such a phase with the separable interaction, we have numerically calculated the 3P_0 superfluid critical temperature as a function of the spin-polarized neutron density. Our result would be useful for further understanding of possible exotic state of matter in neutron stars.

For further quantitative investigations, it is important to study the critical magnetic field of 1S_0 superfluid within the beyond-mean-field theory as well as the model with finite-range interactions. One can also expect a 3P_0 pairing of protons which are dilute even around the core region of a neutron star. In such a case, the Landau quantization plays a crucial role [69]. Moreover, while we have considered homogeneous neutron matter in this study, nuclear clusters would be important as the non-monotonic density dependence of

the S -wave pairing gap has been reported in the presence of the inhomogeneous potential induced by nuclei [70,71]. A proximity effect [72] associated with the topological 3P_0 superfluid can also be expected near the nuclear clusters. Since neutrons inside the nuclei are insensitive to the magnetic field because of the large density compared to the gas phase, the competition between 1S_0 and 3P_0 pairings may occur near the surface of neutron-rich nuclei in the crust.

Note added. When this paper was being finalized, there appeared a preprint [73], where the 3P_0 triplet superfluid in neutron matter is discussed.

Acknowledgments. H.T. thanks K. Sekizawa, K. Iida, Y. Ominato, K. Yoshida, A. Dohi, and the members of H. Liang group for the useful discussion and A. Sedrakian for providing the numerical data in Ref. [15]. N.Y. also thanks H. Okawa and K. Fujisawa for fruitful discussion on the evolutions of neutron stars. The authors thank RIKEN iTHEMS NEW working group for fruitful discussions. This work is supported by Grants-in-Aid for Scientific Research provided by JSPS through Nos. 18H05406, 20K03951, 21H01800, 21H04565, 22H01158, 22K13981, and 23H01839. Y.S. is supported by Pioneering Program of RIKEN for Evolution of Matter in the Universe (r-EMU).

-
- [1] D. Pines and M. A. Alpar, *Nature (London)* **316**, 27 (1985).
 [2] D. J. Dean and M. Hjorth-Jensen, *Rev. Mod. Phys.* **75**, 607 (2003).
 [3] A. Sedrakian and J. W. Clark, *Eur. Phys. J. A* **55**, 167 (2019).
 [4] T. Takatsuka and R. Tamagaki, *Prog. Theor. Phys. Suppl.* **112**, 27 (1993).
 [5] P. Mészáros, D. B. Fox, C. Hanna, and K. Murase, *Nat. Rev. Phys.* **1**, 585 (2019).
 [6] D. Page, M. Prakash, J. M. Lattimer, and A. W. Steiner, *Phys. Rev. Lett.* **106**, 081101 (2011).
 [7] V. G. J. Stoks, R. A. M. Klomp, M. C. M. Rentmeester, and J. J. de Swart, *Phys. Rev. C* **48**, 792 (1993).
 [8] K. D. Marquez, M. R. Pelicer, S. Ghosh, J. Peterson, D. Chatterjee, V. Dexheimer, and D. P. Menezes, *Phys. Rev. C* **106**, 035801 (2022).
 [9] K. Sekizawa and K. Kaba, [arXiv:2302.07923](https://arxiv.org/abs/2302.07923).
 [10] D. Chatterjee, J. Novak, and M. Oertel, *Phys. Rev. C* **99**, 055811 (2019).
 [11] L. Scurto, H. Pais, and F. Gulminelli, *Phys. Rev. C* **107**, 045806 (2023).
 [12] C. Dehman, D. Viganò, S. Ascenzi, J. A. Pons, and N. Rea, *Mon. Not. R. Astron. Soc.* **523**, 5198 (2023).
 [13] K. Makishima, T. Enoto, J. S. Hiraga, T. Nakano, K. Nakazawa, S. Sakurai, M. Sasano, and H. Murakami, *Phys. Rev. Lett.* **112**, 171102 (2014).
 [14] A. A. Isayev and J. Yang, *Phys. Rev. C* **80**, 065801 (2009).
 [15] M. Stein, A. Sedrakian, X.-G. Huang, and J. W. Clark, *Phys. Rev. C* **93**, 015802 (2016).
 [16] T. Mizushima, S. Yasui, D. Inotani, and M. Nitta, *Phys. Rev. C* **104**, 045803 (2021).
 [17] W. Zwerger, *The BCS-BEC Crossover and the Unitary Fermi Gas*, 1st ed., Vol. 836 (Springer, Berlin/Heidelberg, 2012).
 [18] G. C. Strinati, P. Pieri, G. Röpke, P. Schuck, and M. Urban, *Phys. Rep.* **738**, 1 (2018).
 [19] Y. Ohashi, H. Tajima, and P. van Wyk, *Prog. Part. Nucl. Phys.* **111**, 103739 (2020).
 [20] P. van Wyk, H. Tajima, D. Inotani, A. Ohnishi, and Y. Ohashi, *Phys. Rev. A* **97**, 013601 (2018).
 [21] F. Chevy, *Phys. Rev. A* **74**, 063628 (2006).
 [22] A. Schirotzek, C.-H. Wu, A. Sommer, and M. W. Zwierlein, *Phys. Rev. Lett.* **102**, 230402 (2009).
 [23] F. Scazza, G. Valtolina, P. Massignan, A. Recati, A. Amico, A. Burchianti, C. Fort, M. Inguscio, M. Zaccanti, and G. Roati, *Phys. Rev. Lett.* **118**, 083602 (2017).
 [24] P. Massignan, M. Zaccanti, and G. M. Bruun, *Rep. Prog. Phys.* **77**, 034401 (2014).
 [25] H. Tajima, J. Takahashi, S. I. Mistakidis, E. Nakano, and K. Iida, *Atoms* **9**, 18 (2021).
 [26] F. Scazza, M. Zaccanti, P. Massignan, M. M. Parish, and J. Levinsen, *Atoms* **10**, 55 (2022).
 [27] M. Klawunn and A. Recati, *Phys. Rev. A* **84**, 033607 (2011).
 [28] H. Sakakibara, H. Tajima, and H. Liang, *Phys. Rev. A* **107**, 053313 (2023).
 [29] I. Vidaña, *Phys. Rev. C* **103**, L052801 (2021).
 [30] H. Tajima, H. Moriya, W. Horiuchi, E. Nakano, and K. Iida, [arXiv:2304.00535](https://arxiv.org/abs/2304.00535).
 [31] B. Frank, J. Lang, and W. Zwerger, *J. Exp. Theor. Phys.* **127**, 812 (2018).
 [32] L. Rammelmüller, Y. Hou, J. E. Drut, and J. Braun, *Phys. Rev. A* **103**, 043330 (2021).
 [33] M. J. Ku, A. T. Sommer, L. W. Cheuk, and M. W. Zwierlein, *Science* **335**, 563 (2012).
 [34] N. Navon, S. Nascimbene, F. Chevy, and C. Salomon, *Science* **328**, 729 (2010).

- [35] M. Horikoshi, M. Koashi, H. Tajima, Y. Ohashi, and M. Kuwata-Gonokami, *Phys. Rev. X* **7**, 041004 (2017).
- [36] M. Pini, P. Pieri, and G. Calvanese Strinati, *Phys. Rev. B* **107**, 054505 (2023).
- [37] K. Nishimura, E. Nakano, K. Iida, H. Tajima, T. Miyakawa, and H. Yabu, *Phys. Rev. A* **103**, 033324 (2021).
- [38] A. Broderick, M. Prakash, and J. Lattimer, *Astrophys. J.* **537**, 351 (2000).
- [39] P.-A. Pantel, D. Davesne, and M. Urban, *Phys. Rev. A* **90**, 053629 (2014).
- [40] R. B. Wiringa, V. G. J. Stoks, and R. Schiavilla, *Phys. Rev. C* **51**, 38 (1995).
- [41] G. Sarma, *J. Phys. Chem. Solids* **24**, 1029 (1963).
- [42] P. Fulde and R. A. Ferrell, *Phys. Rev.* **135**, A550 (1964).
- [43] A. I. Larkin and Y. N. Ovchinnikov, *Sov. Phys. JETP* **20**, 762 (1965).
- [44] A. Bulgac, M. McNeil Forbes, and A. Schwenk, *Phys. Rev. Lett.* **97**, 020402 (2006).
- [45] P. Magierski, B. Tüzemen, and G. Wlazłowski, *Phys. Rev. A* **100**, 033613 (2019).
- [46] P. Magierski, B. Tüzemen, and G. Wlazłowski, *Phys. Rev. A* **104**, 033304 (2021).
- [47] L. Radzihovsky and D. E. Sheehy, *Rep. Prog. Phys.* **73**, 076501 (2010).
- [48] K. B. Gubbels and H. T. Stoof, *Phys. Rep.* **525**, 255 (2013).
- [49] V. Gurarie, L. Radzihovsky, and A. V. Andreev, *Phys. Rev. Lett.* **94**, 230403 (2005).
- [50] W. J. Gully, D. D. Osheroff, D. T. Lawson, R. C. Richardson, and D. M. Lee, *Phys. Rev. A* **8**, 1633 (1973).
- [51] V. Ambegaokar and N. D. Mermin, *Phys. Rev. Lett.* **30**, 81 (1973).
- [52] D. D. Osheroff and P. W. Anderson, *Phys. Rev. Lett.* **33**, 686 (1974).
- [53] G. E. Volovik, *Lect. Notes Phys.* **718**, 31 (2007).
- [54] L. G. Johnsen, H. T. Simensen, A. Brataas, and J. Linder, *Phys. Rev. Lett.* **127**, 207001 (2021).
- [55] Y. Ominato, A. Yamakage, and M. Matsuo, *Phys. Rev. B* **106**, L161406 (2022).
- [56] H. Funaki, A. Yamakage, and M. Matsuo, *Phys. Rev. B* **107**, 184437 (2023).
- [57] N. Chamel, D. Page, and S. Reddy, *Phys. Rev. C* **87**, 035803 (2013).
- [58] M. Y. Kagan and D. Efremov, *J. Low Temp. Phys.* **158**, 749 (2010).
- [59] L. B. Leinson, *Phys. Lett. B* **741**, 87 (2015).
- [60] M. Kobayashi and M. Nitta, *Phys. Rev. C* **105**, 035807 (2022).
- [61] Y. Masaki, T. Mizushima, and M. Nitta, *Phys. Rev. B* **105**, L220503 (2022).
- [62] T. Luu, M. J. Savage, A. Schwenk, and J. P. Vary, *Phys. Rev. C* **82**, 034003 (2010).
- [63] L. Mathelitsch and B. J. VerWest, *Phys. Rev. C* **29**, 739 (1984).
- [64] V. Gurarie and L. Radzihovsky, *Ann. Phys.* **322**, 2 (2007).
- [65] A. J. Leggett, in *Modern Trends in the Theory of Condensed Matter: Proceedings of the XVI Karpacz Winter School of Theoretical Physics, February 19–March 3, 1979 Karpacz, Poland* (Springer, Berlin, 2008), pp. 13–27.
- [66] M. Prakash, J. M. Lattimer, J. A. Pons, A. W. Steiner, and S. Reddy, *Lect. Notes in Phys.* **578**, 364 (2001).
- [67] D. N. Aguilera, V. Cirigliano, J. A. Pons, S. Reddy, and R. Sharma, *Phys. Rev. Lett.* **102**, 091101 (2009).
- [68] S. Ramanan and M. Urban, *Eur. Phys. J.: Spec. Top.* **230**, 567 (2021).
- [69] D. Allor, P. Bedaque, T. D. Cohen, and C. T. Sebens, *Phys. Rev. C* **75**, 034001 (2007).
- [70] P. Schuck and X. Viñas, *Phys. Rev. Lett.* **107**, 205301 (2011).
- [71] A. Pastore, J. Margueron, P. Schuck, and X. Viñas, *Phys. Rev. C* **88**, 034314 (2013).
- [72] T. Okihashi and M. Matsuo, *Prog. Theor. Exp. Phys.* **2021**, 023D03 (2021).
- [73] E. Krotscheck, P. Papakonstantinou, and J. Wang, [arXiv:2305.07096](https://arxiv.org/abs/2305.07096).